

UNIVERSIDAD DE LOS ANDES

The expected shape of the Milky Way's dark matter halo

by

Jesus David Prada Gonzalez

A thesis submitted in partial fulfillment for the
degree of Master of Sciences in Physics

in the
Faculty of Sciences
Physics Department

April 2018

Declaration of Authorship

I, AUTHOR NAME, declare that this thesis titled, ‘THESIS TITLE’ and the work presented in it are my own. I confirm that:

- This work was done wholly or mainly while in candidature for a research degree at this University.
- Where any part of this thesis has previously been submitted for a degree or any other qualification at this University or any other institution, this has been clearly stated.
- Where I have consulted the published work of others, this is always clearly attributed.
- Where I have quoted from the work of others, the source is always given. With the exception of such quotations, this thesis is entirely my own work.
- I have acknowledged all main sources of help.
- Where the thesis is based on work done by myself jointly with others, I have made clear exactly what was done by others and what I have contributed myself.

Signed:

Date:

“Write a funny quote here.”

If the quote is taken from someone, their name goes here

UNIVERSIDAD DE LOS ANDES

Abstract

Faculty of Sciences
Physics Department

Master of Sciences

by Jesus David Prada Gonzalez

The shape of the Dark Matter (DM) structure (halo) in which a galaxy is embedded is heavily determined by the anisotropic accretion of mass from its specific environment. Therefore, the shape of a galaxy's halo is an important feature to inquire about its formation history and the relation of DM and gas within it. In this work we study the shape of the DM halo of Milky Way-like galaxies from the Auriga simulations. We focus on the radial and time dependence. We found that, on DM-only and Magnetohydrodynamic (MHD) simulations, the shape of the DM halo is more triaxial in the inner-skirts than in the outer-skirts. We compared simulations with and without gas and verified that the presence of visible matter has an effect of rounding the DM halo which is amplified for smaller radii, where the gravitational potential of the galactic disk becomes more significant. Regarding the effect of time on the DM halo shape, we corroborated that it is well-conserved in comoving units until $z \approx 2$. This means that probing the halo shape at the virial radius in physical units for different redshifts is nearly equivalent to probing the shape at different radii at redshift 0. These results are in accordance with previous work on cosmological and galactic-size simulations, and may serve as guidelines to improve observational constraints on our MW DM halo.

UNIVERSIDAD DE LOS ANDES

Abstract

Faculty of Sciences
Physics Department

Master of Sciences

by Jesus David Prada Gonzalez

La forma de la estructura (halo) de Materia Oscura en la cual está embebida una galaxia es altamente determinada por la acreción anisotrópica de materia en el entorno específico en el que ésta se encuentra. Es por esto que la forma del halo de una galaxia es una característica importante para indagar sobre su historia de formación y la relación entre Materia Oscura y gas dentro de ella. En este trabajo estudiamos la forma de los halos de materia oscura en galaxias de tipo Vía Láctea del catálogo de simulaciones Auriga. Nos centramos principalmente en su dependencia radial y temporal. Hemos encontrado, en simulaciones de sólo Materia Oscura y en simulaciones de Magneto-hidrodinámica, que la forma del halo es más triaxial en las partes de adentro que en las afuera. Al comparar simulaciones con y sin gas, verificamos que la presencia de materia visible tiene un efecto de redondeado sobre el halo de Materia oscura, el cual es amplificado en radios pequeños, donde el efecto gravitacional del disco galáctico se torna significante. En cuanto al efecto del tiempo en la forma del halo de Materia Oscura, hemos corroborado que esta se conserva en unidades comóviles hasta $z \approx 2$. Esto se ve reflejado en la aproximada equivalencia entre el muestreo de la forma en el radio virial en unidades físicas a diferentes redshifts y el muestreo a diferentes radios en la actualidad. Estos resultados son respaldados por trabajos previos en simulaciones de escala galáctica y cosmológica, y pueden servir como lineamientos para mejorar las mediciones de la forma del halo de Materia Oscura de nuestra Vía Láctea.

UNIVERSIDAD DE LOS ANDES

Abstract

Faculty of Sciences
Physics Department

Master of Sciences

by Jesus David Prada Gonzalez

Given the elusive nature of Dark Matter (DM), indirect measurements are the most common approach to study it observationally. However, to make these studies possible, some assumptions must be made. These assumptions come from complicated theoretical frameworks and the analysis of state-of-the-art cosmological simulations. In this work we study the shape of the DM halo of Milky Way-like galaxies from the Auriga simulations. We focus on the radial and time dependence. We found that, on DM-only and Magnetohydrodynamic (MHD) simulations, the shape of the DM halo is more triaxial in the inner-skirts than in the outer-skirts. We compared simulations with and without gas and verified that the presence of visible matter has an effect of rounding the DM halo which is amplified for smaller radii, where the gravitational potential of the galactic disk becomes more significant. Regarding the effect of time on the DM halo shape, we corroborated that it is well-conserved in comoving units until $z \approx 2$. This means that probing the halo shape in physical units at the virial radius for different redshifts is nearly equivalent to probing the shape at different radii at redshift 0. These results are in accordance with previous work on cosmological and galactic-size simulations, and may serve as guidelines to improve observational constraints on our MW DM halo.

Acknowledgements

The acknowledgements and the people to thank go here, don't forget to include your project advisor...

Contents

Declaration of Authorship	i
Abstract	iii
Resumen	iv
Abstract MOCCA	v
Acknowledgements	vi
List of Figures	ix
List of Tables	x
Abbreviations	xi
Physical Constants	xii
Symbols	xiii
1 Introduction	1
1.1 About Dark Matter	1
1.2 Theoretical background for DM	3
1.3 Constraining the Milky Way's DM Halo	6
1.4 State of the art on MW simulations	8
1.5 Synergy between Theory, Observations and Simulations	11
1.6 Outline	12
2 Remarks about our study	13
2.1 The Auriga simulations	13
2.2 Determining the halo shape	15
3 Our results	18
3.1 Analysis of convergence	18

3.2	The shape's radial dependence	21
3.2.1	The effect of gas on the halo shape	22
3.3	Historical shape	23
4	Conclusions	33
A	An Appendix	34

List of Figures

2.1	Set of 30 MW-like simulations from Auriga, taken from http://auriga.h-its.org/	14
3.1	Examples of halos where level 3 (pink) and level 4 (green) calculations are in good agreement.	20
3.2	Examples of halos that have an appreciable difference between level 3 (pink) and level 4 (green) calculations.	25
3.3	Comparison of the effect of resolution on DM and MHD simulations. Here level4 curves (magenta) are compared to the mean and 2std (confirm) of the random-sampled curves from level3. For better comparison of the effect of resolution, the difference percent is plotted in green.	26
3.4	Example of the dependence of shape in terms of the radius. All graphics have matching orientation (which may not be the same) with their respective principal axes at the shown radii. The horizontal and vertical axes are aligned to the major and medium semi-axes respectively.	27
3.5	Semi-axial ratios and triaxiality $\frac{1-b/a}{1-c/a}$ as function of radius for semi-axes $a \geq b \geq c$. The MHD simulation (blue dotted line) shows ratios closer to 1 than those from the DM-only (green solid line) simulation. The rounding effect with radius for each simulation separately is also well-appreciable in this graphic. The radial-rounding, as well as the gas-presence amplification can be evidenced on the triaxiality function.	28
3.6	General tendency on the triaxial plane c/a Vs b/a . Some observational constraints (stars and error-bar point) are plotted alongside our results . .	29
3.7	General tendency on the triaxial plane c/a Vs b/a . Some observational constraints (stars and error-bar point) are plotted alongside our results . .	30
3.8	Example of historic shape conservation in comoving coordinates.	31
3.9	Example of historic shape disruption in comoving coordinates. The consistency between MHD and DM implies some major-event like a close merger or a collision. The non-continuous red line corresponds to a very close moment of this merging event, which is amplified in MHD.	32

List of Tables

- 2.1 Specifications of each level 4 galaxy (halo). The DM and MHD versions of each parameters are presented together. The columns of this table indicate: (1) Halo name, (2,3) Number of (millions) of DM particles belonging to the halo, (4,5) Mass per particle in $10^5 M_\odot$, (6,7) Virial radius (R TopHat 200) of the halo in Kpc, (8,9) Virial mass of the halo in $10^{14} M_\odot$. 15
- 2.2 Specifications of each level 3 galaxy (halo). The DM and MHD versions of each parameters are presented together. The columns of this table indicate: (1) Halo name, (2,3) Number of (millions) of DM particles belonging to the halo, (4,5) Mass per particle in $10^5 M_\odot$, (6,7) Virial radius (R TopHat 200) of the halo in Kpc, (8,9) Virial mass of the halo in $10^{14} M_\odot$. 16

Abbreviations

LAH List Abbreviations Here

Physical Constants

Speed of Light c = $2.997\ 924\ 58 \times 10^8$ ms⁻¹ (exact)

Symbols

a	distance	m
P	power	W (Js ⁻¹)
ω	angular frequency	rads ⁻¹

For/Dedicated to/To my...

Chapter 1

Introduction

1.1 About Dark Matter

In the field of observational astronomy it is very plausible to encounter ourselves with indirect or direct measurements which are not reconcilable with the current understanding of physical theories. Very often, these intriguing measurements are the result of inaccuracy in the measurement device or the assumption of some erroneous or non-precise premises. However, since the early beginings of the 20th century, we have found inconsistencies of observations with the accepted paradigm of physics, which have been reliably proven not to arise from any errors in the premises or devices. These inconsistent measurements principally question the veracity of the Newtonian gravity or even its improved Einsteinian version at astronomical and cosmological scales.

The principal problem of these inconsistencies can be resumed to the fact that we observe that objects are moving in a certain way that cannot be explained exclusively by the effect of gravitational forces of visible matter. In fact, there is very strong historical evidence that this gravitational effect is heavily *underestimated* if we only take into account the effect of light-interacting matter. To solve this problem without blaming the measurement instruments or the used premises, which have been consistently ruled out as the sources of these discrepancies, there are two important hypothesis to study.

One of these hypothesis, which is the most simple to understand, tries to reconcile these observations with Newtonian gravity, or even more, General Relativity, assuming it is completely valid in the cosmological context. Consequently, if there is nothing wrong with the theoretical framework, the premises, nor the instruments, and gravitational effects cannot be explained solely with the matter that we observe, then there must exist

some kind of matter that exerts this missing gravitational pull, which we cannot see for some reason. We talk about Dark Matter (DM).

Since early as the 1930's, the DM hypothesis has been considered. It is known that Fritz Zwicky proposed the presence of some kind of DM within the Coma cluster of galaxies to explain the cluster attachment despite the galaxy's huge velocities that would have made them escape [?]. At first, this proposal was not given much attention as there were many other sources of errors to blame, and these observations were not widely replicated. Nevertheless, as years passed, more and more inconsistencies could be explained with the use of this DM hypothesis. It is the case of the famous rotation curves [?] where the amount of visible matter on galaxies could not account for the centripetal acceleration associated with the tangential velocities of stars within it. It is, in essence, the argument of Zwicky. Later on, with a better understanding of the space-curving effect of matter predicted by general relativity and the improvement of precision in telescopes, it was possible to measure weak lensing (gravitational distortion of observed objects) through massive clusters of galaxies [?]. Again, this effect was estimated to be much more dim compared to the actual result of observations, suggesting the existence of DM. This is, in fact, a naturally different approach than those of velocity-curves analysis.

Less direct evidence of DM include arguments related to structure formation and the observed Cosmic Microwave Background Radiation (CMBR) [?]. On one hand, the structure formation argument is based in the fact that the early stages of the universe were dominated by radiation, which heavily affects visible matter by preventing it to grow clumps from small density anisotropies. Specifically, due to radiation the speed of sound at the early stages of the universe is very close to that of the speed of light, meaning that density anisotropies must be quite large for them to not be dispersed as sound waves. These anisotropies would be evidenced on the CMBR as temperature fluctuations. It has been thoroughly corroborated that these anisotropies are not present on a very precise sampling of the CMBR like WMAP [?] and PLANCK [?]. In the absence of any other kind of pulling force or kind of matter with smaller speed of sound (unaffected by radiation), such as DM, we would not have the same distribution of collapsed structures we observe today (stars, galaxies, clusters) as these density fluctuations would have been dispersed as sound waves.

Subsequently, the second important hypothesis to reconcile observations with our theoretical framework is of opposing nature than that of DM. In this case, we study the

possibility that the General Theory of Relativity is not accurate and is in fact underestimated at cosmological scales. We talk in this case of Modified-Newtonian Dynamical (MOND) theories. This is a natural consequence of assuming that the universe is what we observe and there is no such thing as non-visible matter. If we apply this hypothesis to the previously presented problems solved with the assumption of the existence of DM, under a precise tuning of parameters of these new theories, we could obtain the sought consistency. However, the problem arises when we try to satisfy this consistency for all observational discrepancies. In the case of DM, many of the observational mismatches with theory may be simultaneously solved and it is possible to make predictions. In the case of MOND theories, many results as rotation curves may be emulated to certain extent [?], but given its strong claims, it is sometimes impossible to reconcile with observations [?]. Actually, these theories are extremely well constrained for small-scale regimes by Newtonian/Einsteinian Gravity, which restricts the freedom with which these models may be adjusted to observations, to such an extent that sometimes a remnant of DM is needed to completely concile the theory with observation [?].

For these reasons, DM is the most widely accepted hypothesis to account for these observational discrepancies. Nonetheless, a complete physical picture of DM is still missing and it is one of the biggest puzzles to fully understand the composition of our Universe. Many appealing candidates may be found in the context of Particle Physics, which motivate the existence different kinds of weak-interacting particles through interesting symmetry-seeking theories [?].

1.2 Theoretical background for DM

In this search for the candidate particle that makes up DM, there have been various proposals from particle physics. One of the most obvious candidates was the neutrino, a lepton of extremely small mass at rest. When physicists studied this option, they discovered that, although it would make sense in principle, there were many problems that suggested that this was not the correct candidate. These arguments come from the analysis of CMB and Structures of Formation and are related to the conclusion that at early stages of the universe, specifically before the decoupling of radiation and matter, neutrinos would be relativistic [?], which would result in a non-hierarchical model of formation. Other arguments include constraints on the number of neutrinos surrounding a galaxy [?]. This kind of very-light DM candidates whose thermal energy may significantly affect the proper growth of density anisotropies in the early universe, are

known as Hot Dark Matter (HDM).

If we assume the existence of a heavier particle as a DM candidate, then these particles would not be relativistic before decoupling and therefore it would support a hierarchical model of formation [?]. In this case, we reffer to this particles as Cold Dark Matter (CDM) as their thermal energy is negligible to analyse the collapse of matter. Given its consistency with the observable universe, CDM is the most accepted candidate as a constituyent of DM.

Given CDM has negligible thermal energy, it is usually modeled as a set of collisionless particles (minimum cross-section) with gravitational interaction, or, in the continuous case, as an ideal collisionless self-gravitating fluid following the Boltzmann equations (1.1). This collisionless feature together with the exclusivity of the gravitational interaction is traduced in a fluid/particle without sense of scale. This means that neither the fluid/particle nor its interaction force possess a well-defined univocal scale parameter. In other words, by a simple rescaling of position and time, we would arrive to a similar system. This characteristic of self-similarity is an extremely important feature of CDM which is widely used on theoretical frameworks as consistent assumptions to simplify the calculations and imply that, at least in a CDM-only universe, many properties of DM structures are self-similar. For instance, on one hand, Schechter et al. used this argument to analyze the statistics of mass functions in a self-similar universe of DM [?] which has proven to be atoundingly precise for observations. On the other hand, Bardeen et al. used this argument to analyze the evolution of random Gaussian fluctuations of the DM density field [?], resulting in a theoretical framework that is a strong foundation for anyone intending to work on the analysis of DM structures.

$$\frac{d\rho}{dt} = \frac{\partial\rho}{\partial t} + \vec{v} \cdot \frac{\partial\rho}{\partial\vec{x}} - \frac{\partial\Phi}{\partial\vec{x}} \cdot \frac{\partial\rho}{\partial\vec{v}}. \quad (1.1)$$

By means of example, using a computational approach, Navarro et al. discovered that DM halos (galactic sized clusters of DM) are rided by a universal double-power law (1.2) dependent on two parameters, namely (r_s, δ_c) . This result was demonstrated to be independent of the size of the halo or the used cosmology [?]. This is to expect from the self-similarity properties of DM, although it differs from the previously theoretically predicted single-power law [?].

$$\frac{\rho(r)}{\rho_{crit}} = \frac{\delta_c}{(r/r_s)(1+r/r_s)^2}. \quad (1.2)$$

Now, the collisionless models for CDM may also be applied as a good approximation for star dynamics or to model other cosmological objects with negligible cross-section according to their extreme low densities on the universe, such as Black Holes (BH). By ways of example, we can take the Boltzmann transport equation (1.1) in a convenient set of coordinates. For instance, we take this collisionless self-gravitating fluid equation in spherical coordinates to analyze the dynamics of stars in axisymmetric galaxies. Now, to get rid of the difficult phase-space density distribution function $f(\vec{x}, \vec{v})$ we conveniently integrate the multiplication of the Boltzmann equation with a power of a velocity component, over the velocity space. The result of this integration is the expresion of the collisionless fluid in terms of more observable quantities such as the velocity means $\bar{v}_r, \bar{v}_z, \bar{v}_\phi$, the velocity correlation matrix σ and the density field ρ and the gravitational accelerations a_r, a_z, a_ϕ . These equations are called Jean's equations in honor of James Jean who was the first to apply this knowledge in the cosmological context [?]. For the case of an axisymmetric stable system [?], these equations read:

$$a_r = \sigma_{rr}^2 \frac{\partial \ln \nu}{\partial r} + \frac{\partial \sigma_{rr}^2}{\partial r} + \sigma_{rz}^2 \frac{\partial \ln \nu}{\partial z} + \frac{\partial \sigma_{rz}^2}{\partial z} + \frac{\sigma_{rr}^2}{r} - \frac{\sigma_{\phi\phi}^2}{r} - \frac{\bar{v}_\phi^2}{r} \quad (1.3)$$

$$a_z = \sigma_{rz}^2 \frac{\partial \ln \nu}{\partial r} + \frac{\partial \sigma_{rz}^2}{\partial r} + \sigma_{zz}^2 \frac{\partial \ln \nu}{\partial z} + \frac{\partial \sigma_{zz}^2}{\partial z} + \frac{\sigma_{rz}^2}{r}, \quad (1.4)$$

where the angular acceleration is null for stability reasons. And the the spatial density ρ is encoded in the stellar number density distribution ν .

In this case, we modelled stars as a collisionless fluid in the presence of a gravitational potential Φ which produces the corresponding accelerations. These accelerations may be obtained by the integration of visible matter, but, as expected, it is underestimated. In this case we have a precise theoretical framework to deduce, given the stellar observable properties, what its the discrepancy in accelerations and in this way calculate the missing distribution of DM.

1.3 Constraining the Milky Way's DM Halo

So far, DM presence can only be measured through its gravitational effect on the surrounding visible matter. One of best the astronomical systems that can be used to probe DM on astronomical scales is our own galaxy: the Milky Way (MW). Probing the DM density field around our galaxy (it's so-called DM halo) can shed light on the nature of DM [? ?] and our galaxy's formation history [? ? ?].

DM haloes have two important features that could be constrained. On one hand there is the density profile, which has been demonstrated to follow an approximately universal model (1.2) [?]. On the other hand, there is the halo shape, which is directly related to its spin. According to the hierarchical model of structure formation, due to the anisotropic history of accretion DM haloes are triaxial and therefore, their shape and spin are important characteristics to **diagnose** their formation history [?].

In this sense, it is of special interest to constrain the DM halo shape of the only cosmological object of which we have a tridimensional view from inside: our Milky Way. However, this is a very difficult labour given the observational restrictions of observation. Many approaches have been made to constrain the MW's DM shape. One of them is to make use of theoretical models that relate the content of matter of our galaxy with the gravitational potential.

For example, Loebman et al. [?] used the axisymmetric Jean's equations [?] that relate the stellar content of our galaxy, with the radial and axial accelerations. The observed accelerations cannot be completely explained by visible matter only and DM presence is needed. Loebman et al. estimated that, around 20Kpc, the DM halo must be perfectly oblate with axis ratio of $q_{DM} = 0.47 \pm 0.14$ to account for this discrepancy.

Nevertheless, the axial symmetry that characterizes this halo is inherited from the use of axisymmetric Jean's equations. Although this is a strong assumption, a more general theoretical background is much more difficult to implement given the difficulty to obtain the needed data from observations. Even authors aknowledge that "... while it is premature to declare $q_{DM} = 0.47 \pm 0.14$ as a robust measurement of the dark matter halo shape, it is encouraging that the simulation is at least qualitatively consistent with SDSS data in so many aspects". This demonstrates that this field of study is still very young and any calculated constraint may lead us to a better understanding of our MW's DM halo shape.

A more common and strong approach is to use the streams of close dwarf galaxies that have been deformed by the gravitational potential of the MW. This effect is very important because the torque generated by the anisotropy in our halo is sensible to its parameters and thus, these streams are strong evidence to constrain the shape of our MW's DM halo [?]. In fact, it is known that a static axisymmetric halo cannot simultaneously explain all the features of the Sagittarius leading arm **citaa**.

In this context Law and Majewski 2010 proposed an analytical model of the MW consisting of a fixed analytical gravitational potential formed by a Miyamoto-Nagai [?] disk, a Hernquist spheroid and a logarithmic halo. This halo is triaxial and is characterized by its axial ratios and orientation. Given all these parameters, the Sagittarius stream was simulated and evolved forward and backwards in time for various choices of the halo parameters. The best fit, compared to a detailed study of the observational properties of the Sagittarius stream, was found at a minor/major axis ratio $(c/a)_\Phi = 0.72$ and intermediate/major axis ratio $(b/a)_\Phi = 0.99$. The minor axis of this triaxial halo was found to be pointing in some direction contained in the galactic disk plane.

This sophisticated model succeeded at simultaneously reproducing the radial velocity and angular position trends of the Sagittarius leading arm, which were troublesome to model with simpler approaches. Nevertheless, the coexistence of a triaxial DM halo and an axisymmetric galactic disk is not supported by Cold Dark Matter (CDM) models [?]. Specifically, it is expected that the DM and gas distributions are correlated in the sense that matter is accreted similarly as is DM, being the interaction properties the principal difference in the behaviour. Having this into account, gas and DM must have aligned angular momenta to certain extent because all kinds of matter are expected to be accreted from the same cosmic structures. In other words, it is expected for minor axes to be rather aligned. Furthermore, due to stability reasons and a historical interaction, the matter distribution should be non-axisymmetric in the presence of a non-axisymmetric halo potential.

Law & Majewski comment in their paper: "... by no means do they (results) represent best-fit models in a statistical sense. Therefore, the predictions made cannot be considered exclusive or definitive but serve to guide where future observations could focus to distinguish between various models.". Particularly, this discrepancy with the current CDM paradigm may be a feature of the specific model. Other important observational constraints were dismissed in this study, such as the non-symmetric influence of the Large Magellanic Cloud (LMC). This feature may obviate the triaxial halo and produce

a more CDM-consistent model. However, observationally obtaining the detailed information of the LMC needed for this kind of research is extremely difficult.

Studies of this kind are by nature non-conclusive(deterministic?, not so conclusive?) due to the difficulty in obtaining precise information from observations. In observations, we take 2-dimensional snapshots of the sky and therefore, we loose resolution of the radial density field due to screening. This makes the process of obtaining a tridimensional view of a cosmological-scale object an extremely difficult endeavour. Furthermore, we can determine radial velocities with doppler effect, but there is no obvious way of obtaining tangencial velocities. Bearing this in mind, any study which is sensible to very detailed observational parameters for obtaining non-direct measurements of the DM density field will be either non-conclusive for reasonable-difficulty models (as is the process of constraining), or must be extremely sophisticated to achieve a significantly conclusive result.

1.4 State of the art on MW simulations

To address this specific difficulty of obtaining information from observations, there is a vast and important field consisting in the modeling of the non-linear behaviour of matter. This is with the objective of numerically simulating the universe at a wide range of scales and produce consistent systems of which we have full control of their parameters at all stages. In this sense, a computer may become a virtual cosmological-scale laboratory, where we may run an experiment having full control over its initial conditions to compare different outputs and support theoretical frameworks.

Cosmological simulations are usually restricted to modelling DM as a non-collisional fluids (1.1) and gas as an Eulerian collisional fluids (??) whose thermal effects are important. Efficiently solving these systems of non-linear equations, specially the ones for an Eulerian fluid, is an intricate puzzle and it is still an open and improving field of research. Difficulties in the numerical modeling of these fluids arise from numerical instabilities and the wide range of values that quantities take in the context of cosmological objects, which can expand in several orders of magnitude, are no much different than actual field discontinuities which are very difficult to treat in a numerical way. It is clear that these simulations are limited to some resolution depending on the current computing power. This resolution is variable between simulations and is adjustable to the specific objective of the research.

In a historical context, numerical astrophysics have experienced a parallel growth with computing power and numerical methods. As we stated earlier, collisionless fluids are not restricted to the modeling of DM but can also be applied to cosmological objects with negligible cross-section. In this sense, as early as 1960's, with the huge advances in computation, it became possible for theoretical astrophysicists to run small-sized simulations of two-dimensional galaxies. This is the case of Miller and Pendergast [?] and Quirk [?] who tried to recover the spiral stable form of galaxies like our MW. At this point in history, the computational power was not sufficient to even attempt a proper solution of collisional fluids. This is a task that requires extreme care and computational power even today. Therefore, to simulate the important thermal effects of collision of gas clouds they emulated temperatures as random peculiar velocities of particles and implemented some cooling process in which some particles lose energy. With this work, and some insight from Jerry Ostriker [?] it was demonstrated that galactic disks cannot be stable on their own and need some sort of additional radial pull (DM). In these simulations it was also verified that spiral branches of galaxies are a consequence of the propagation of small density fluctuations driven by dissipation of energy by gas clouds (particles). However, it was later demonstrated by Tomre & Tomre [?] that these anisotropies could also be caused by tidal forces of close encounters between galaxies.

$$\frac{d\rho}{dt} + \rho \vec{\nabla} \cdot \vec{v} = 0 \quad (1.5)$$

$$\frac{d\vec{v}}{dt} = -\frac{\vec{\nabla}P}{\rho} - \vec{\nabla}\Phi \quad (1.6)$$

$$\frac{du}{dt} = -\frac{P}{\rho} \vec{\nabla} \cdot \vec{v} - \frac{\Lambda(\vec{u}, \rho)}{\rho} \quad (1.7)$$

$$P = (\gamma - 1)\rho u \quad (1.8)$$

Even with the advances of computational power each two years following Moore's law, the numerical methods used to solve simulations quickly became obsolete year by year and needed to be pushed forward to an optimization of the computational resources and numerical resolution. In this way, computational astrophysics evolved from brute-force N^2 -body simulations to the use of tree-based simulations [], mesh-based simulations [] and even dynamical-mesh simulations []. This co-evolution between numerical methods and astrophysics, together with the exponential growth of computational power, eventually made possible the performance of Cosmological-sized DM-only simulations such as Millennium which could reproduce the observed cosmological structures.

In this context of precise CDM-consistent DM-only simulations, the analysis of gas was usually imprinted through the use of semi-analytic methods that took the output numerical density field and performed analytical calculations to match the distribution of a certain number of visible-matter properties that we observe today [?]. Although these semi-analytical methods did not trace the evolution of gas alongside with DM throughout the simulation, it was the most realistic model that could be performed to do a proper analysis of gas. By this time, numerical methods trying to actually simulate gas suffered from a process of over-cooling in which gas collapsed too quickly and did not produce stable galaxy-sized disk like we observe today [?].

This over-cooling process was understood to be a consequence of not having into account events of energy transportation that redistributed energy through the gas stopping this rapid collapse. The principal sources of this energy transport are now known to be supernovae (SN) explosions, radiation from cosmic rays and the Active Galactic Nucleus (AGN). These terms are usually referred to as stellar feedback, radiation pressure and AGN feedback, respectively. They enclose modern physics processes which cannot be fully simulated due to the computational limitations and must be estimated with general recipes with some free parameters. For instance, in case of SNe explosions this process of energetic feedback is simulated by isotropically liberating some amount of kinetic energy (radial velocity recoil) as well as some amount of thermal energy (Temperature), to the surrounding gas cells.

A decade ago, these feedback processes were not as well understood nor well modeled as they are today. For this reason, and the advances in technology, it has been possible only until recently the simulation of an unprecedented set of 30 galactic-sized objects like our MW, tracing the evolution of normal matter alongside with DM with exceptional accuracy. This project is called Auriga, [?] and not only it has state-of-the-art energetic feedback physics which do not need recalibration of parameters in terms of resolution unlike other less consistent approaches, it is run with the novel hydrodynamic code AREPO [?]. This code combines a moving Voronoi tessellation with the finite volume approach and in this way, it solves the principal sources of numerical errors from both important paradigms of computational hydrodynamics in the cosmological context. Moreover, it is the first time that a consistent Magnetic Field could be simulated in these kind of simulations [?].

1.5 Synergy between Theory, Observations and Simulations

In the CDM paradigm, we have fully theoretical studies [? ?] principally focused in the analysis of Gaussian random fields and the properties of self-similarity that DM must possess. These theoretical frames are then supported by CDM simulations [?] and, if possible, by observations. In fact, these theories are usually thoroughly verified and complemented through simulations, given their convenient malleability, before being directly applied to observations.

One good example of this synergy between analytical models, numerical simulations and observational data is evidenced in the work of Vera-Ciro et al. (2011-2013). In 2011, Vera-Ciro et al. studied the shape of a set of four simulated MW-like DM galaxies with the objective of complementing the predictions of the CDM paradigm. Specifically, the hierarchical model of structure formation predicts that the halo shape is correlated with the environment given that it determines the structures from which it accretes matter [?]. However, theoretical studies of halo shapes are restricted to the correlations at redshift 0 and do not say much about their history of formation. Intuitively, it is expected that halo shapes vary with the radius taking into account that accretion occurs at progressively bigger radii in history and that the cosmic structures that determine environments evolve during that time. Due to the collisionless nature of DM, inner shells can interact with outer shells only in a gravitational way. This means that the historical shape is somewhat conserved in the radial shape profile.

Vera-Ciro et al. showed in 2011 that the radial profile of the halo shape is indeed correlated with its accretion history and environment. Furthermore, due to the increase in the cross section of the halos, which contributes to the scattering of particles, at later stages and bigger radii, they become more oblate/spherical. These results helped to obtain more insight about the galactic dynamics of formation and also suggested some guidelines to improve Law & Majewski 2010 study.

In 2013, Vera-Ciro et al. proposed an improved study based on the one by Law & Majewski in 2011. Vera-Ciro et al. proposed a halo that is perfectly oblate at inner regions and transitions smoothly to a triaxial halo in the outer-skirts. With this, the angular momentum inconsistency of this constraint with the CDM model is solved. They found that this halo is triaxial in the outer skirts with a medium-to-major axis ratio of 0.9

and minor-to-major axis of 0.8, which is still very oblate regarding the CDM predictions.

However, even when this study solves some inconsistencies with the expected predictions, it demonstrated that small perturbations are important. That is, even when the Sagittarius stream samples the gravitational potential at the outer parts of the halo, where the shape of the inner regions should not be so important, the outer shape is affected to compensate for the change in the regions from inside. This effect takes our attention to a relegated topic: the LMC. In fact, Vera-Ciro et al. demonstrated that the change in shape from the inner regions produces a torque comparable to that of the LMC, which should be taken into account in further researches.

This section must end emphasizing that we will perform our study based on this previous work on Auriga simulations.

1.6 Outline

Set the outline of the thesis.

Chapter 2

Remarks about our study

In this chapter describe in detail the specifications of the simulations we are going to work with. Furthermore, we present the chosen method for determining the halo shapes. This chapter is mainly to thoroughly explain how are we going to do everything that we are going to do.

2.1 The Auriga simulations

In this monograph we use the results of the state-of-the art Auriga simulations [?]. It selected a set of 30 isolated halos from the Eagle simulations [?]. Each halo was identified with a modified version of the algorithm "Friend of Friends" (FOF) [?], that recursively links particles if they are closer than some distance threshold called linking length. Eagle follows the evolution of fixed-mass particles of $m_{\text{DM}} = 1.15 \cdot 10^7 M_{\odot}$ from $z = 127$ to $z = 0$. Eagle simulations adopt the cosmological model from Planck Collaboration et al. (2014) by taking the parameters $\Omega_{\Lambda} = 0.693$, $\Omega_m = 0.307$, $\Omega_b = 0.048$ & $H_0 = 67.77 \text{km s}^{-1} \text{Mpc}^{-1}$.

These halos were randomly selected from a sample of the quartile of most isolated halos whose virial mass M_{200} varied between $10^{12} M_{\odot}$ and $2 \cdot 10^{12} M_{\odot}$. This mass is defined as the mass enclosed within the virial radius R_{200} at which the density becomes 200 times the critical density of the universe. These halos were then re-simulated by increasing the mass resolution of the particles belonging to each halo and diminishing the resolution of the rest of the particles. This would efficiently simulate external gravitational effects over the studied structure and reproduce a high-resolved version of it.

Various versions of the same halo were simulated for different degrees of realism. All 30 halos were simulated within a level 4 degree of resolution defined for Aquarius simulations which corresponds to $\tilde{3} \cdot 10^6$ high resolution particles of $\tilde{2.5} \cdot 10^5 M_\odot$. The principal details of each of these halos are consigned on the table 2.1. From these halos, 6 of them were re-simulated at level 3 (higher) resolution taking into account a spatial factor of 2 in each dimension. For more information about level 3 halos, their information is printed on table 2.2. Furthermore, for each halo in each level of resolution there are two versions of the simulation. One evolves only DM particles and the other has into account all the magneto-hydrodynamical physics, including DM. Taking this into account, we can compare the results from different levels of realism to obtain consistency in our analysis.

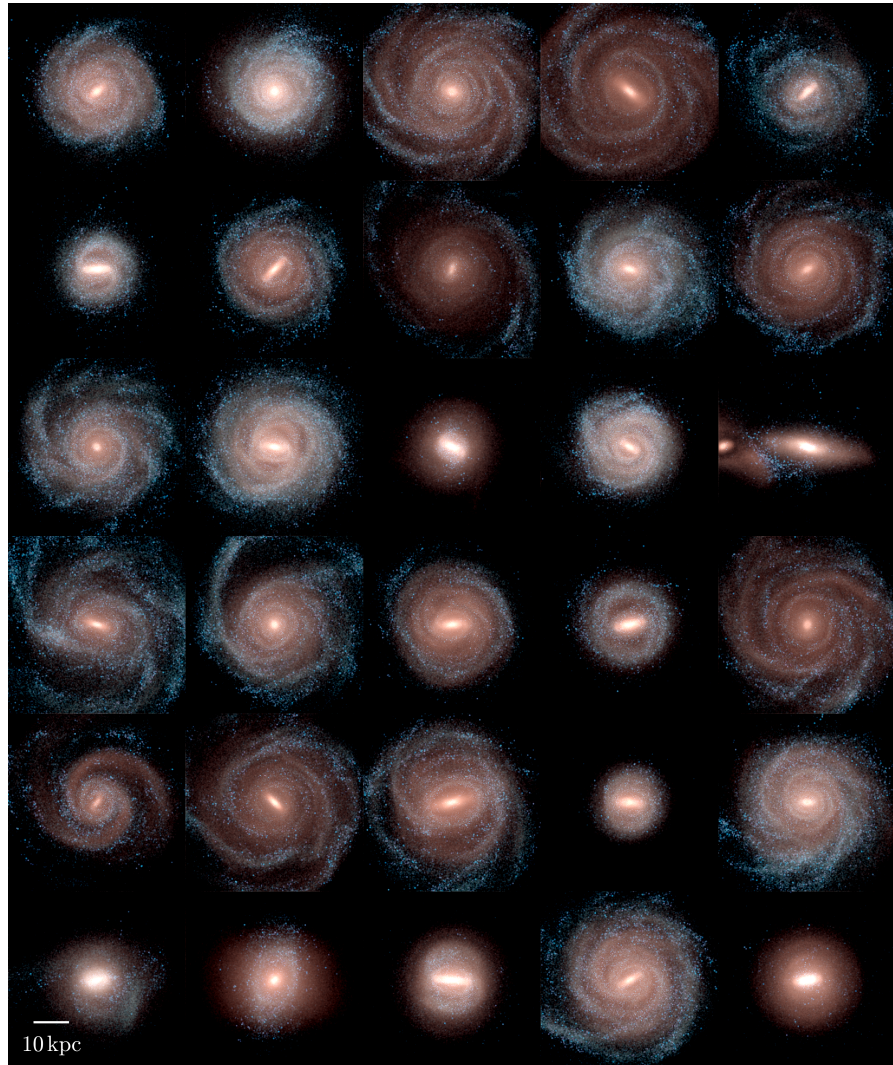


FIGURE 2.1: Set of 30 MW-like simulations from Auriga, taken from <http://auriga.h-its.org/>

Halo	$N_P/10^6$		$M_P/10^5 M_\odot$		R_{vir}/Kpc		$M_{vir}/10^{14} M_\odot$	
	DM	MHD	DM	MHD	DM	MHD	DM	MHD
halo 1	4.068	2.447	2.397	2.022	196.927	187.674	9.062	7.844
halo 2	5.625	5.457	2.481	2.093	235.094	233.934	15.418	15.191
halo 3	3.826	3.852	2.645	2.231	210.693	210.955	11.099	11.141
halo 4	4.585	4.530	2.590	2.185	219.378	215.438	12.529	11.866
halo 5	3.262	3.290	2.533	2.137	196.984	197.246	9.071	9.106
halo 6	3.184	3.110	2.337	1.972	191.840	189.342	8.378	8.054
halo 7	3.878	3.729	2.296	1.937	197.864	196.509	9.193	9.005
halo 8	2.772	2.796	2.451	2.068	190.716	191.764	8.231	8.368
halo 9	3.038	3.010	2.738	2.310	195.826	190.640	8.911	8.222
halo 10	2.700	2.751	2.541	2.144	187.139	188.147	7.777	7.904
halo 11	4.146	4.116	2.541	2.144	221.821	219.568	12.952	12.560
halo 12	2.865	2.908	2.645	2.231	192.280	192.038	8.436	8.404
halo 13	3.520	3.600	2.393	2.019	202.139	203.815	9.801	10.048
halo 14	4.200	4.475	2.499	2.108	215.535	218.927	11.882	12.453
halo 15	2.888	2.845	2.541	2.144	199.848	200.658	9.471	9.588
halo 16	3.821	3.871	2.499	2.108	212.590	212.632	11.401	11.408
halo 17	2.752	2.781	2.552	2.153	188.067	187.404	7.893	7.811
halo 18	3.770	3.624	2.738	2.310	201.124	207.293	9.655	10.571
halo 19	2.989	3.086	2.645	2.231	200.244	200.325	9.527	9.540
halo 20	3.903	3.822	2.481	2.093	210.097	211.423	11.005	11.214
halo 21	4.105	4.075	2.640	2.227	219.527	219.823	12.555	12.604
halo 22	2.794	2.766	2.625	2.215	188.363	184.801	7.931	7.489
halo 23	3.977	4.073	2.795	2.358	217.768	215.959	12.254	11.952
halo 24	4.466	4.426	2.522	2.127	217.440	215.147	12.199	11.817
halo 25	2.902	2.806	2.645	2.231	199.922	198.299	9.482	9.254
halo 26	4.610	4.716	2.506	2.115	219.984	218.939	12.633	12.454
halo 27	5.060	5.018	2.590	2.185	228.036	226.225	14.071	13.740
halo 28	4.184	4.276	2.645	2.231	216.979	217.997	12.121	12.294
halo 29	4.827	4.613	2.499	2.108	225.791	219.935	13.660	12.625
halo 30	3.268	3.112	2.579	2.176	195.043	194.741	8.805	8.763

TABLE 2.1: Specifications of each level 4 galaxy (halo). The DM and MHD versions of each parameters are presented together. The columns of this table indicate: (1) Halo name, (2,3) Number of (millions) of DM particles belonging to the halo, (4,5) Mass per particle in $10^5 M_\odot$, (6,7) Virial radius (R TopHat 200) of the halo in Kpc, (8,9) Virial mass of the halo in $10^{14} M_\odot$.

2.2 Determining the halo shape

The discretization of the DM density field into particles makes it difficult to perform some calculations that would require a more continuous distribution such as those related to the density field. The case of the shape of the halo is no exemption, and therefore there is no trivial way to calculate the DM halo shape at a determined radius. There are different approaches to this problem, such as the use of an inertia tensor or the approximation to the respective contour surface. However, the results do

Halo	$N_P/10^6$		$M_P/10^5 M_\odot$		R_{vir}/Kpc		$M_{vir}/10^{14} M_\odot$	
	DM	MHD	DM	MHD	DM	MHD	DM	MHD
halo 6	24.902	24.185	0.292	0.246	191.741	188.367	8.365	7.932
halo 16	29.750	30.334	0.312	0.263	212.622	212.542	11.406	11.395
halo 21	31.993	31.503	0.330	0.278	219.731	220.250	12.588	12.679
halo 23	31.379	31.618	0.349	0.295	217.793	213.358	12.259	11.524
halo 24	34.987	35.153	0.315	0.266	217.313	213.963	12.179	11.624
halo 27	39.617	39.056	0.324	0.273	227.908	223.484	14.048	13.244

TABLE 2.2: Specifications of each level 3 galaxy (halo). The DM and MHD versions of each parameters are presented together. The columns of this table indicate: (1) Halo name, (2,3) Number of (millions) of DM particles belonging to the halo, (4,5) Mass per particle in $10^5 M_\odot$, (6,7) Virial radius (R TopHat 200) of the halo in Kpc, (8,9) Virial mass of the halo in $10^{14} M_\odot$.

not vary very much from method to method [?]. In this work we follow the guidelines by Vera-Ciro et al 2011 which includes the use of the shape method by Allgood 2006[?].

Allgood's method starts with particles enclosed within a sphere whose radius r is the initial radius where we want to obtain the shape. We calculate the reduced inertia tensor:

$$I_{ij} = \sum_k \frac{x_k^{(i)} x_k^{(j)}}{d_k^2}, \quad (2.1)$$

which has weighted components by distance $d^2 = x^2 + y^2 + z^2$, so that each particle contribute with same importance to the inertia tensor, neglecting their distance to the center of the halo.

The diagonalization of this tensor yields the principal axes of the structure, as well as the eigen-quantities $a > b > c$ which produce the respective axial ratios. However, if we characterize an ellipsoid taking into account only particles enclosed within a sphere, we are effectively underestimating its triaxiality [?]. For this reason, we iteratively recalculate the inertia tensor taking into account the previously characterized ellipsoid.

AllGood et al. propose to use the eigenvalues $a > b > c$ and their respective eigen-axes v_a, v_b, v_c to recalculate the inertia tensor over the particles enclosed by the ellipsoid with principal axes (along the respective eigenvectors) equal to $r, r/q, r/s$, where ere $q = b/a$ and $s = c/a$ are the axial ratios. In other words, we repeat the process of calculating the inertia matrix by taking into account particles within an ellipsoid with axial ratios

given by the previous diagonalization, maintaining the principal axis of the enclosing ellipsoid constant (this is a freedom choice).

This method sounds good and it would eventually converge to a more accurate characterization of the halo ellipsoid. However, we are computing the reduced inertia tensor by weighting the contributions with the spherical-metric distance $d^2 = x^2 + y^2 + z^2$, where particles within the same spherical surface are given the same importance. This means we are again underestimating ??? the triaxiality of the structure. For this reason, on each iteration we must calculate the inertia tensor taking into account an elliptic metric: $\bar{d}^2 = x^2 + y^2/q^2 + z^2/s^2$, assuming x, y, z are the corresponding principal axes.

In case this concept of an elliptic metric is difficult to grasp, let us consider that, instead of converting the initial enclosing sphere to the halo ellipse, we are converting the halo ellipsoid into an sphere by performing scale transforms along the respective eigen-axes. From this point of view, we start our first-guess calculation of the ellipsoid by calculating the reduced inertia tensor (2.1) for particles enclosed within a sphere of radius r . Then with the results of this first guess, we perform the following scale transform:

$$(x, y, z) \rightarrow (x', y', z') = (x, y/q, z/s) \quad (2.2)$$

$$q = b/a$$

$$s = c/a,$$

where we assumed the axes x, y, z are oriented at the principal axes. We then repeat the process of calculating the reduced inertia tensor and performing the scale transform until we achieve certain convergence criterion. We stop this iterative process when the sum of the fractional change in axes is less than 10^{-6} to obtain the shape of the halo at the geometric mean radius $(abc)^{1/3}$, which is not much different from the initial radius.

Notice that calculating the inertia tensor with the scaled coordinates x', y', z' is equivalent to calculating it with the un-scaled coordinates x, y, z but using the elliptic-metric distance $\bar{d}^2 = x^2 + y^2/q^2 + z^2/s^2$, for diagonalization purposes.

Chapter 3

Our results

In this chapter we are going to present our results. First some remarks about resolution and convergence of the shape within Auriga simulations for DM and MHD. Then we study the radial and historic profiles of DM and MHD halos, where we obtain the expected tendency found by Vera-Ciro et al. 2011. Then present our principal results, which are the ones referring the comparison DM-MHD.

3.1 Analysis of convergence

One of the principal factors that may bias our study is the resolution of the simulations we work with. Fortunately, Auriga simulations have level 3 and level 4 versions of 6 of the galaxies which we can use to serve our purposes. This a tool principally thought to analyze the numerical convergence of the methods used to solve the non-linear equations for matter and give validity over the output results overall. However, resolution may also directly affect our procedure for calculating halo shapes through the reduction of particles taken into account to calculate the inertia tensor.

To illustrate this, in figures 3.1 we compare the obtained halo shape at redshift 0 on level 3 and level 4 simulations for a halo in which resolution does not noticeably affect the results. In this case, we can say that there is good convergence of the studied quantities with very small numerical bias. However, this is not the case every simulated halo as they do not evolve similarly and some resolution-sensitive events may influence their history of formation.

By way of example, in figures 3.2 we present one of the halos where resolution played the most appreciable role affecting the shape. In this case, although the difference is not extreme, it requires attention and a more careful analysis.

For instance, by simple inspection, we notice that there is no apparent systematic way in which resolution affects the halo shape. That is, sometimes the halo appears rounder and some times it is affected towards a more triaxial shape. This is important for our study as we focus our efforts on the analysis of the triaxial properties of the halo. Incidentally, the DM-only halos remain unchanged with the exemption of the radial regimes where the number of particles naturally affects our shape-calculating method. However, for MHD simulations, the resolution of gas influences the measurement not only in the inner parts, where discretization issues are evident, but it has a more global effect. We suspect this is caused by the scattering of particles due to dense structures formed by gas, whose effect is affected by resolution. Nevertheless, further calculations need to be performed to confirm if these resolution biases are directly caused by AllGood's method for calculating shapes, or are caused because structures are indeed affected by numerical errors from the solution of fluid equations of matter.

Consequently, we decided to isolate the few-particle effect on our shape calculations without recurring to the less-resolved simulations of level 4. Taking into account that the resolution difference between level 3 and level 4 simulations is a factor of 8 in the number of DM particles, we randomly selected particles from level 3 halos at redshift 0 to produce 10 samples of approximately the same size as level 4 simulations. We then proceeded to analyze the effect of lowering the number of particles on the calculated shape of the halo. In figures 3.3 we plotted the original level 3 shapes as well as the 10 level 3 samples. For each radius, we calculated the standard deviation of the sample shape and illustrated 3-sigma range to compare with the respective level 4 shape values.

From the graphics on 3.3, it is clear that the plotted fractional difference is not actually big and remains under 1% for the majority of the radial profile. It becomes important for radii less than $1Kpc$ due to the lack of particles for approximating an elliptical shape. This is corroborated by the 3σ range, which also becomes evident around $1Kpc$. We then deduce from this convergence analysis that for radii bigger than $1Kpc$, the differences of level 3 and level 4 ellipses cannot be explained as an effect of the lack of particles. This is a confirmation that all kinds of matter are directly affected by resolution due to precision-sensitive events on the history of formation or because the

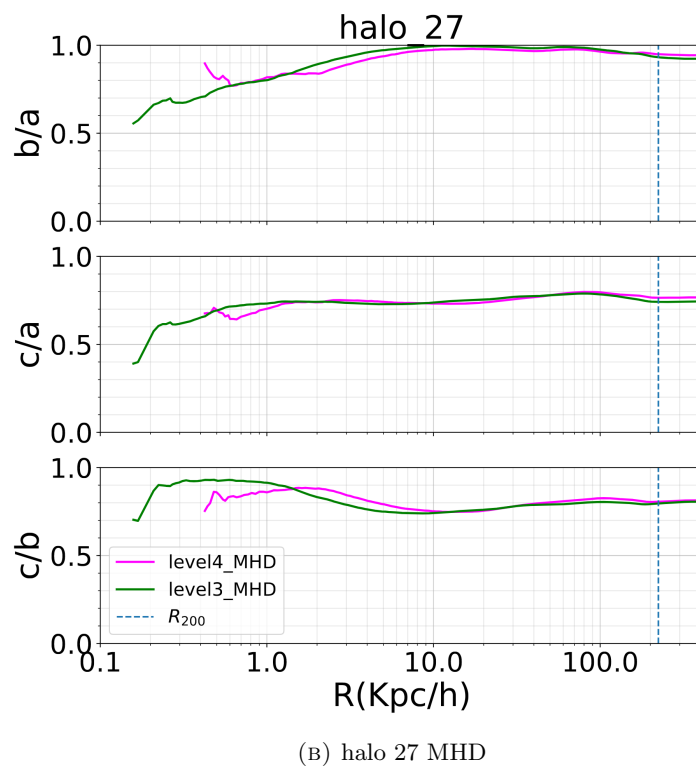
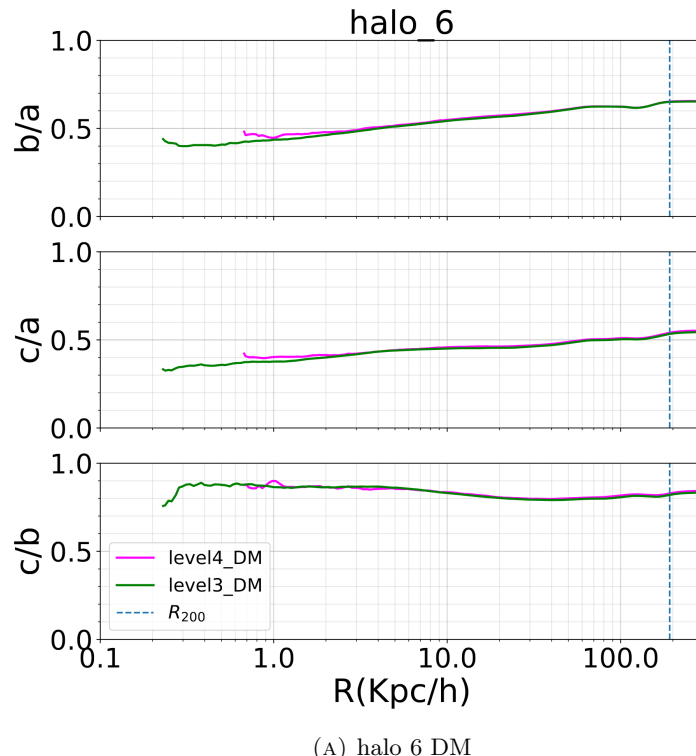


FIGURE 3.1: Examples of halos where level 3 (pink) and level 4 (green) calculations are in good agreement.

numerically calculated gravitational potential of matter itself is affected and continuously influences surrounding structures. Either way, even for the most resolution-biased cases, we can say that for the purposes of this study, convergence is achieved to a reasonable extent.

3.2 The shape's radial dependence

One of the first results we obtained in this study is related to the evolution of the DM halo shape in terms of the radius at which it is sampled. We already expect from previous work that the shape does not remain constant along the radius [?]. Specifically, we know that halos are gradually constructed from inner shells to outer shells through the accretion of matter from cosmic structures []. Inner shells are shielded from the gravitational potential from outer regions as a consequence of the Gauss law. Therefore, inner shells tend to conserve their shape. Outer shells, on the other side, are affected by the increasing gravitational potential from the inside of the halo, which makes them prone to scattering effects. This scattering of particles has a "rounding" effect on the outskirts shape. For this reason, we expect on both simulations (MHD and DM) that halos are more triaxial on inner regions and more spherical at bigger radii. This effect has been corroborated on multiple cosmological simulations (Citas)[].

In figures 3.4, we present a halo in which the rounding effect is specially evident for both degrees of realism (Horizontal comparison). However, to eliminate any possible qualitative bias, we present a more detailed and quantitative version of this effect in terms of the radius on figure 3.5. There, we include all axial ratios, which clearly become closer to 1 (more spherical) for bigger radii. Besides the axial ratios, we included a quantification of the triaxiality, namely $T = \frac{1-b/a}{1-c/a}$.

This measurement T tends towards unity when the medium-to-major axis ratio becomes equal to the minor-to-major ratio, i.e. when the halo becomes prolate. In the case where the medium axis is very close to the major axis, having a different minor axis, T tends to a null value, i.e. when the halo tends to an oblate shape. In these terms, halos are expected to be more prolate on the inside and more oblate on the outside. Even though the perfect spherical shape has a divergent/undefined T value, prolate shapes are associated with triaxial characterizations and oblate shapes are identified as approximately spherical shapes. This, however, can be confirmed on the triaxiality plane where we can

also demonstrate that this is in fact a global tendency on all halos.

In figure 3.6, we show the axial ratios on the plane $c/aVsb/a$. There, each dot represents a specific halo shape at a specific radius. In this plane, oblate halos are represented by the vertical line $x = 1$, prolate halos are identified on the identity line and spheres are exactly the point $(1, 1)$. This gives us a broader idea of the evolution of the shape than a single number T . In this figure, the tendency is clear for DM and MHD halos to get rounder with increasing radius. In fact, the difference in shape clear enough that it is possible to identify groups in case the radius label is lost.

3.2.1 The effect of gas on the halo shape

We have simultaneously corroborated the rounding effect of radius on the halo shape from DM-only and MHD simulations. However, from the parallel presentation of both of the results, it is easily noticeable that there is also a relation of this rounding effect in terms of the presence of matter, which is to be expected [?].

Unlike DM, gas collapses and generate disks which are much denser than the DM structures. This amplifies scattering events and, if we apply the same logic, we would expect that the inner regions of the halo are more spherical when there is presence of gas. We expect the same for outer regions but this effect is predicted to be more significant due to the stronger effect of the gravitational potential of gas on the outer shells.

For instance, recurring again to the figures 3.4, now comparing the graphics vertically, the rounding effect of visible matter is clear. For a more quantitative illustration of this, we can refer to figure 3.5.

Although from previous pictures it is evident that the presence of gas affects the halo shape by rounding it, it is not clear that this effect is amplified for bigger radii. To confirm this, we reappear again to triaxiality plane on 3.7, where this tendency becomes evident.

So far, our results are in accordance with previous work on different kinds of simulations. Nonetheless, on the specific case of MW-like galaxy simulations, we have confirmed the expected tendency in an unprecedented statistically significant sample of 30 galaxies

form Auriga, compared to the 4-sample galaxies from the previous state-of-the art DM-only Aquarius simulations. Moreover, we confirmed that these results are sustained for the specific case of novel MHD MW-like galaxy simulations.

3.3 Historical shape

Taking into account the previously explained model of formation of halos as a qualitative theoretical background that supports our results, it is possible to extend its reach not only for refshift 0 predictions but for the analysis of the historical evolution of the halo shape [].

Recalling that inner shells of the halo are isolated from the gravitational effect of outer shells, the only source of disruption in time of this radial regime are external cosmic structures that perform some torque on them. Outer shells must feel this source of deformation too in addition to the effect of scattering from the inner gravitational potential. Consequently, we expect a systematic change on the halo shape with time, which becomes more significant for bigger radii.

Major events, like mergers, may completely disturb a galaxy shape and erase any memory of it. However, from $z \approx 1$ onwards, these events are very rare [] and we expect that any source of disruption is weak and is reduced to the previously mentioned factors. These sources of anisotropy and scattering randomize DM particle orbits producing a more spherical version of the halo. []

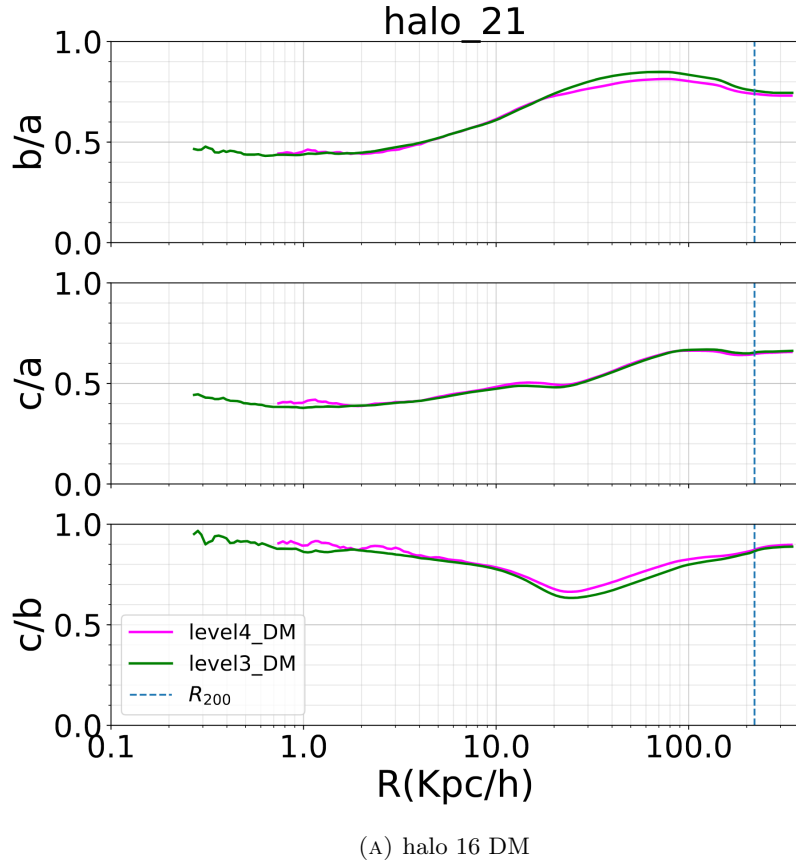
In figures 3.8 we present the evolution of the radial profile of the shape of a halo that managed to conserve its integrity until $z \approx 2$. In this case, we present our results in terms of the comoving coordinates to make these profiles comparable. The halo becomes systematically more spherical as it evolves in time, being this effect more relevant for $r > 50Kpc$.

In figures we present a very special case of a halo that was perturbed at some time around $z = 0.5$. It is specially evident because of the discontinuity caused in the radial profile and the large differences in the different virial radii.

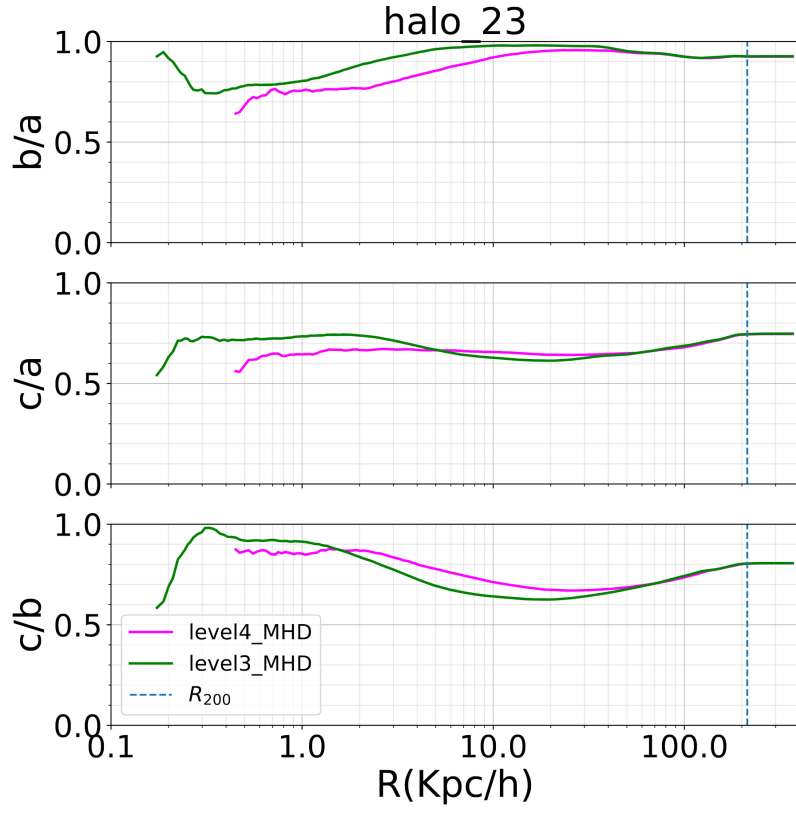
Now, these results compare radial profiles in comoving coordinates, but in real life we have physical coordinates. In this order of ideas, we can state this conservation of the shape (obviating the rounding effect) without recurring to comoving comparisons.

In this case, let us consider a physical radius R that is well-defined for each redshift. It is the radius at which we are going to perform our historical measurements. For practical purposes let us take, for example, the virial radius at each redshift. Then, as halos are continuously accreting matter, the virial radius will be in general smaller (in comoving, just as means of comparison) for higher redshifts. This means we are effectively sampling the shape for smaller radii at higher redshifts. Taking into account that the halo shape is well conserved in time, we expect that studying the historical profile of the shape at a certain constant physical radius is nearly equivalent to studying the radial profile of the same halo at the present time.

To illustrate this, in figures ?? we present the historical and radial profiles of the previously analyzed halo shapes. For the halo that maintained a consistent shape during time, there is a clear correlation between the historical and radial profiles, both clearly tending to more spherical shapes at lower redshifts and bigger radii. In the case of the halo that had a major disrupting event, this correlation is not clear, however, a diffuse tendency to rounder shapes still remains.



(a) halo 16 DM



(b) halo 23 MHD

FIGURE 3.2: Examples of halos that have an appreciable difference between level 3 (pink) and level 4 (green) calculations.

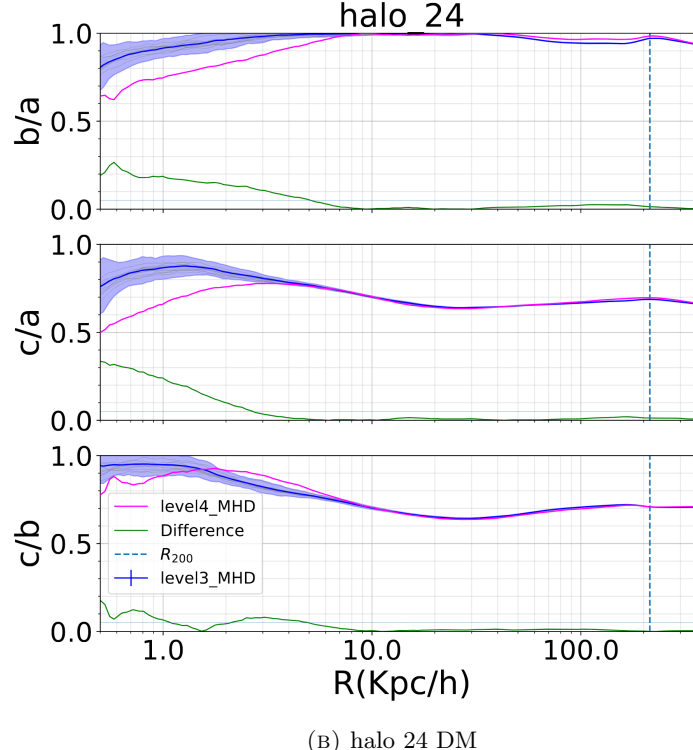
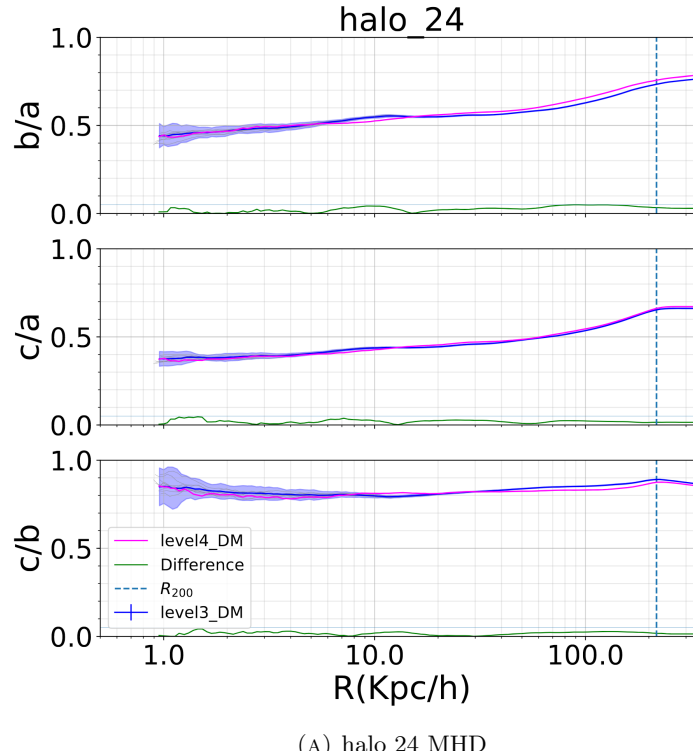


FIGURE 3.3: Comparison of the effect of resolution on DM and MHD simulations. Here level4 curves (magenta) are compared to the mean and 2std (confirm) of the random-sampled curves from level3. For better comparison of the effect of resolution, the difference percent is plotted in green.

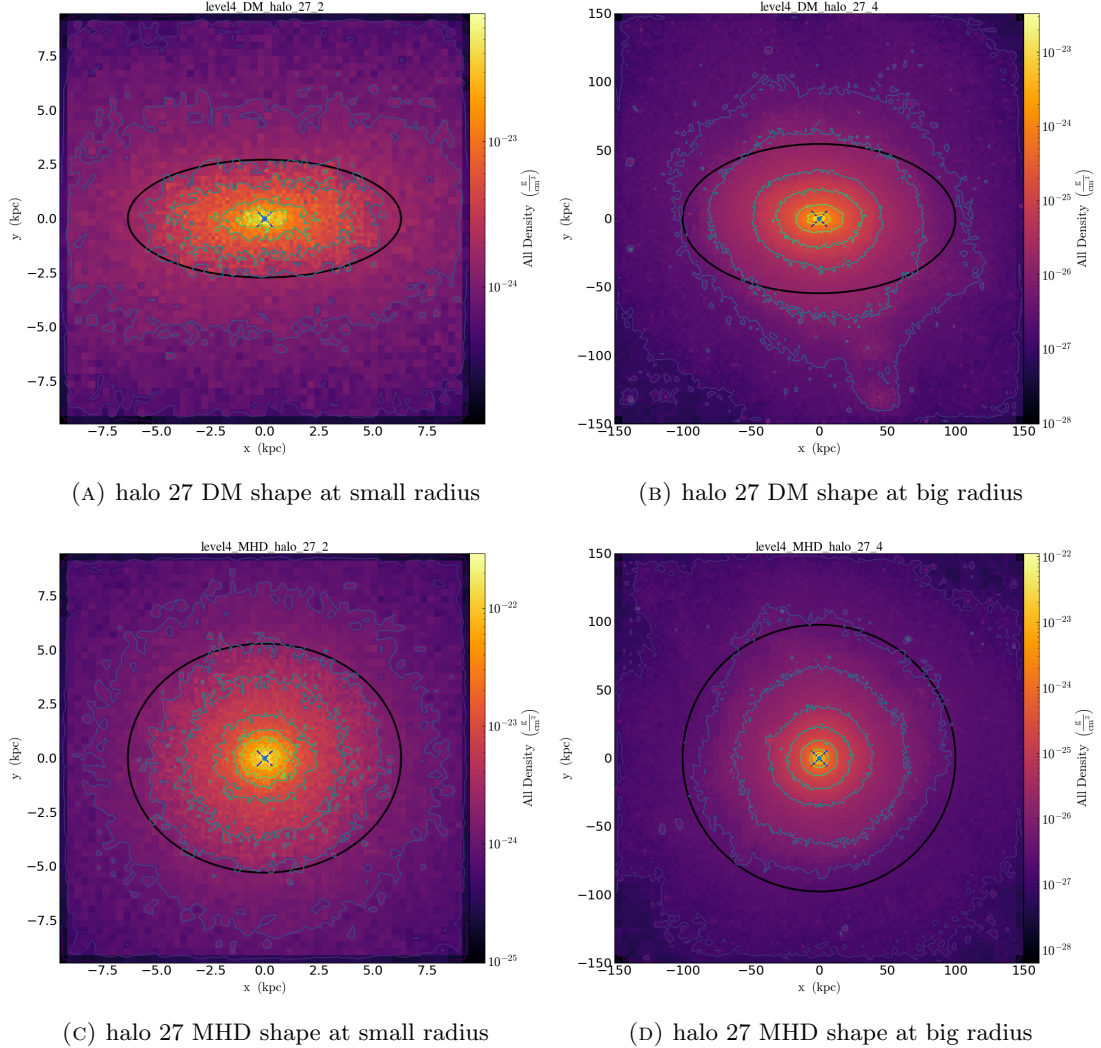


FIGURE 3.4: Example of the dependence of shape in terms of the radius. All graphics have matching orientation (which may not be the same) with their respective principal axes at the shown radii. The horizontal and vertical axes are aligned to the major and medium semi-axes respectively.

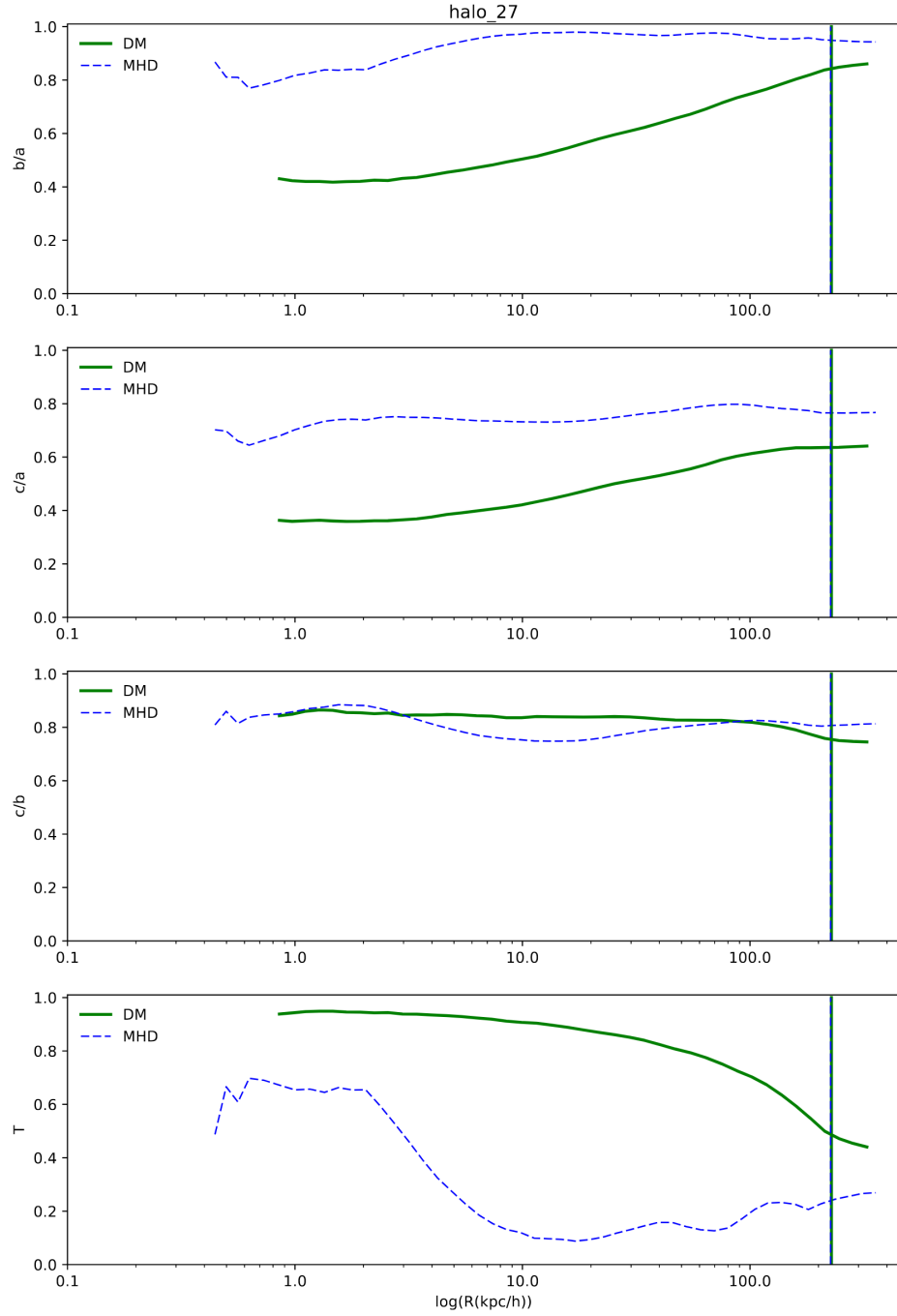


FIGURE 3.5: Semi-axial ratios and triaxiality $\frac{1-b/a}{1-c/a}$ as function of radius for semi-axes $a \geq b \geq c$. The MHD simulation (blue dotted line) shows ratios closer to 1 than those from the DM-only (green solid line) simulation. The rounding effect with radius for each simulation separately is also well-appreciable in this graphic. The radial-rounding, as well as the gas-presence amplification can be evidenced on the triaxiality function.

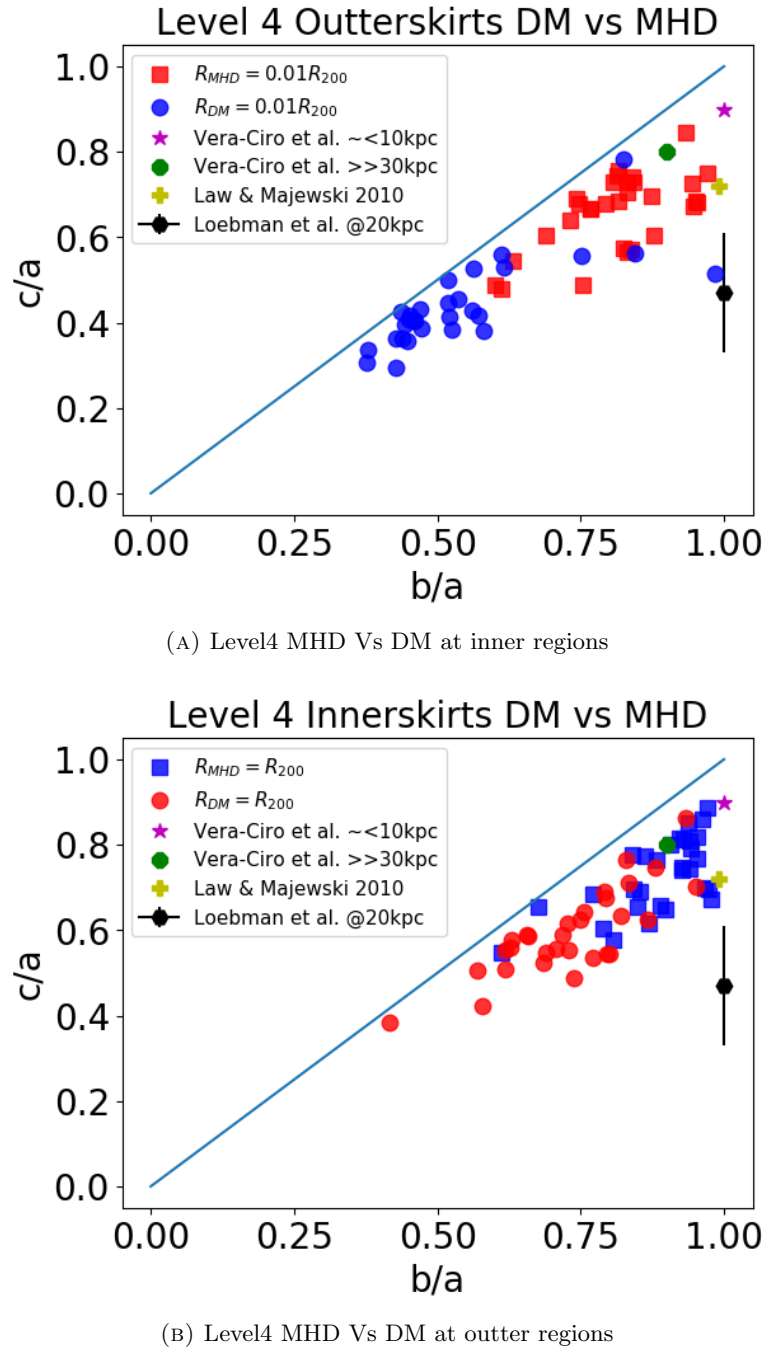


FIGURE 3.6: General tendency on the triaxial plane c/a Vs b/a . Some observational constraints are plotted alongside our results

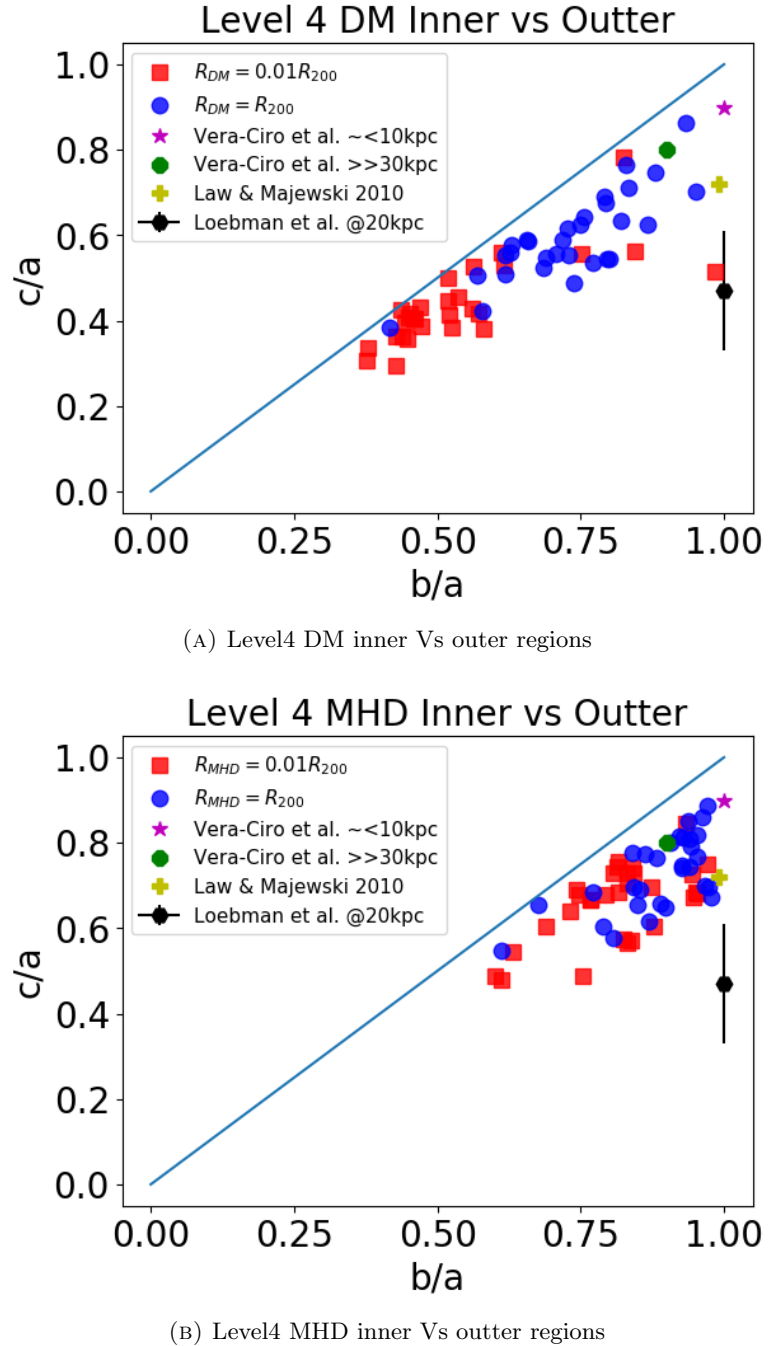


FIGURE 3.7: General tendency on the triaxial plane c/a Vs b/a . Some observational constraints are plotted alongside our results

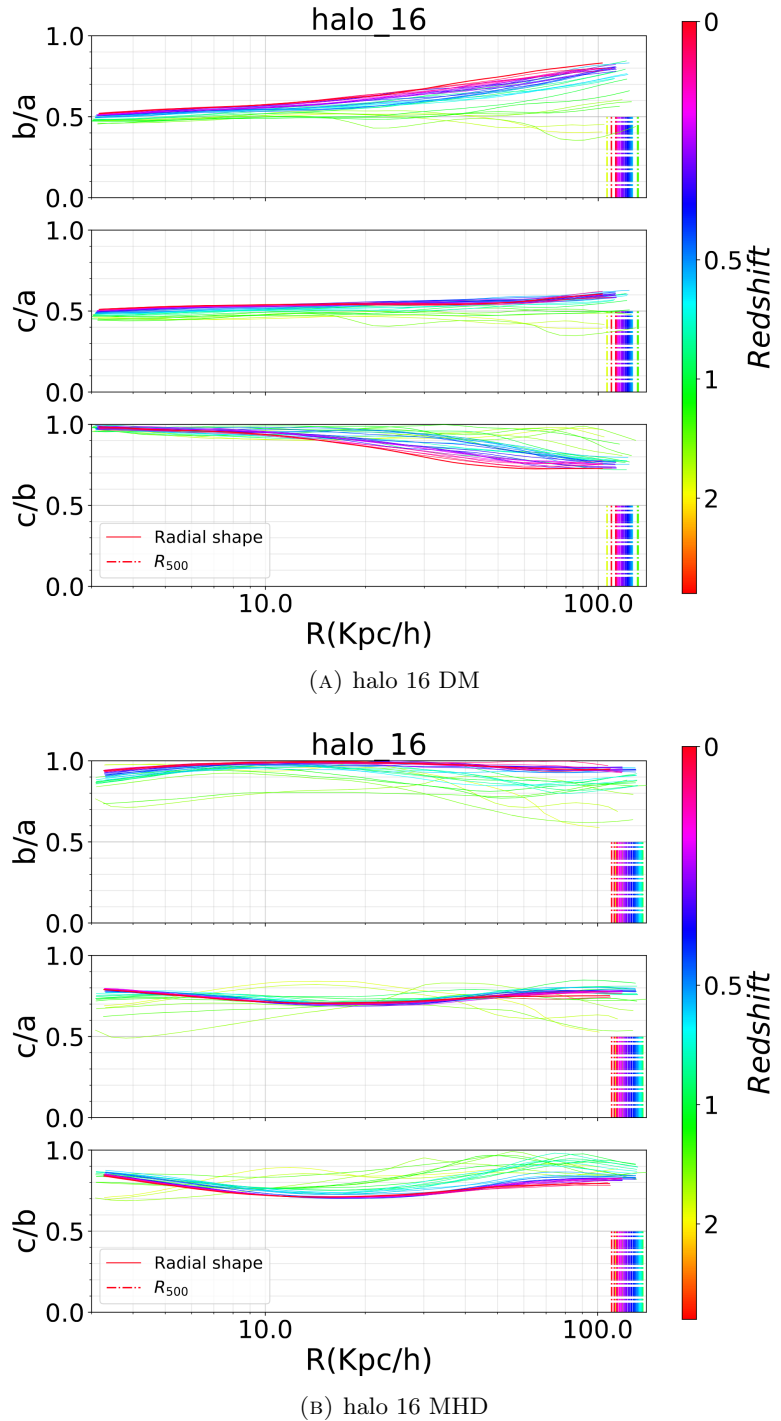


FIGURE 3.8: Example of historic shape conservation in comoving coordinates.

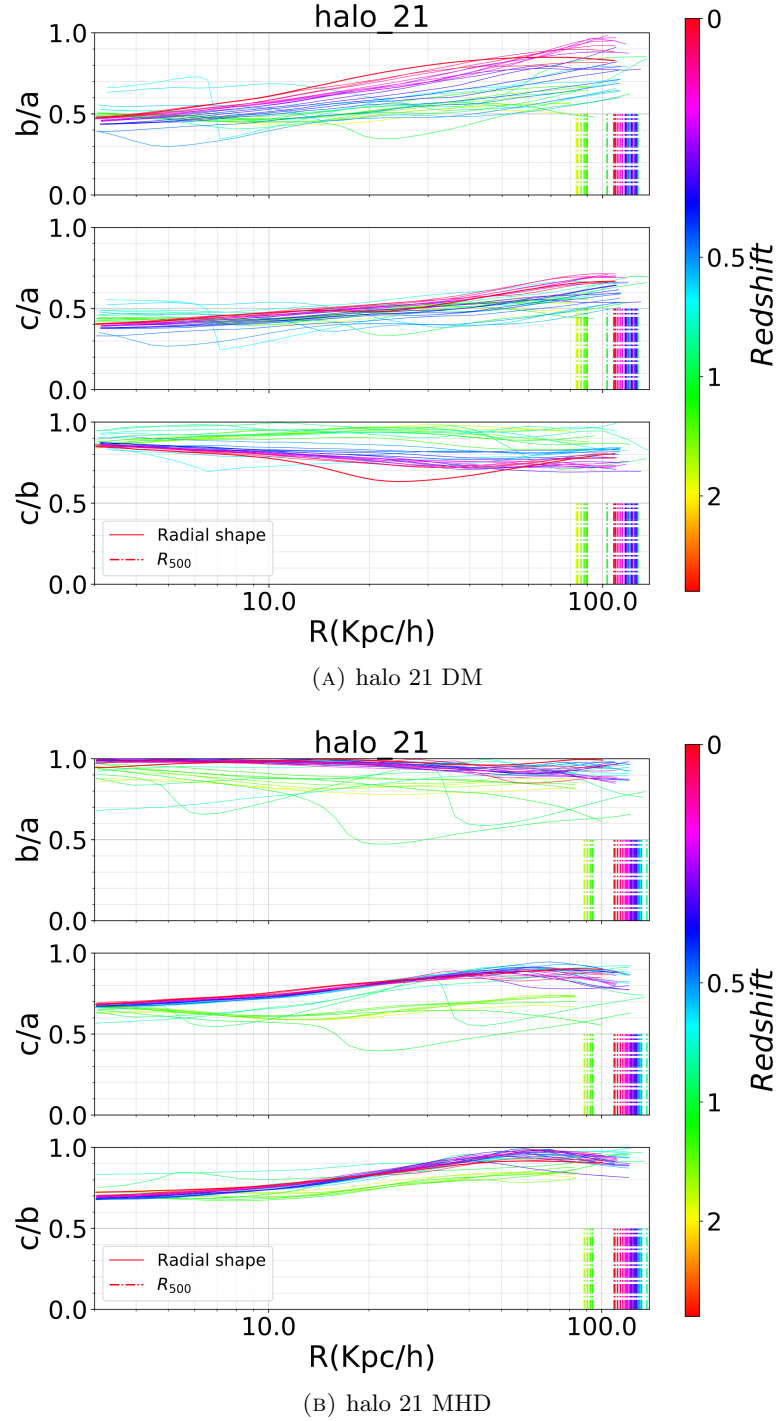


FIGURE 3.9: Example of historic shape disruption in comoving coordinates. The consistency between MHD and DM implies some major-event like a close merger or a collision. The non-continuous red line corresponds to a very close moment of this merging event, which is amplified in MHD.

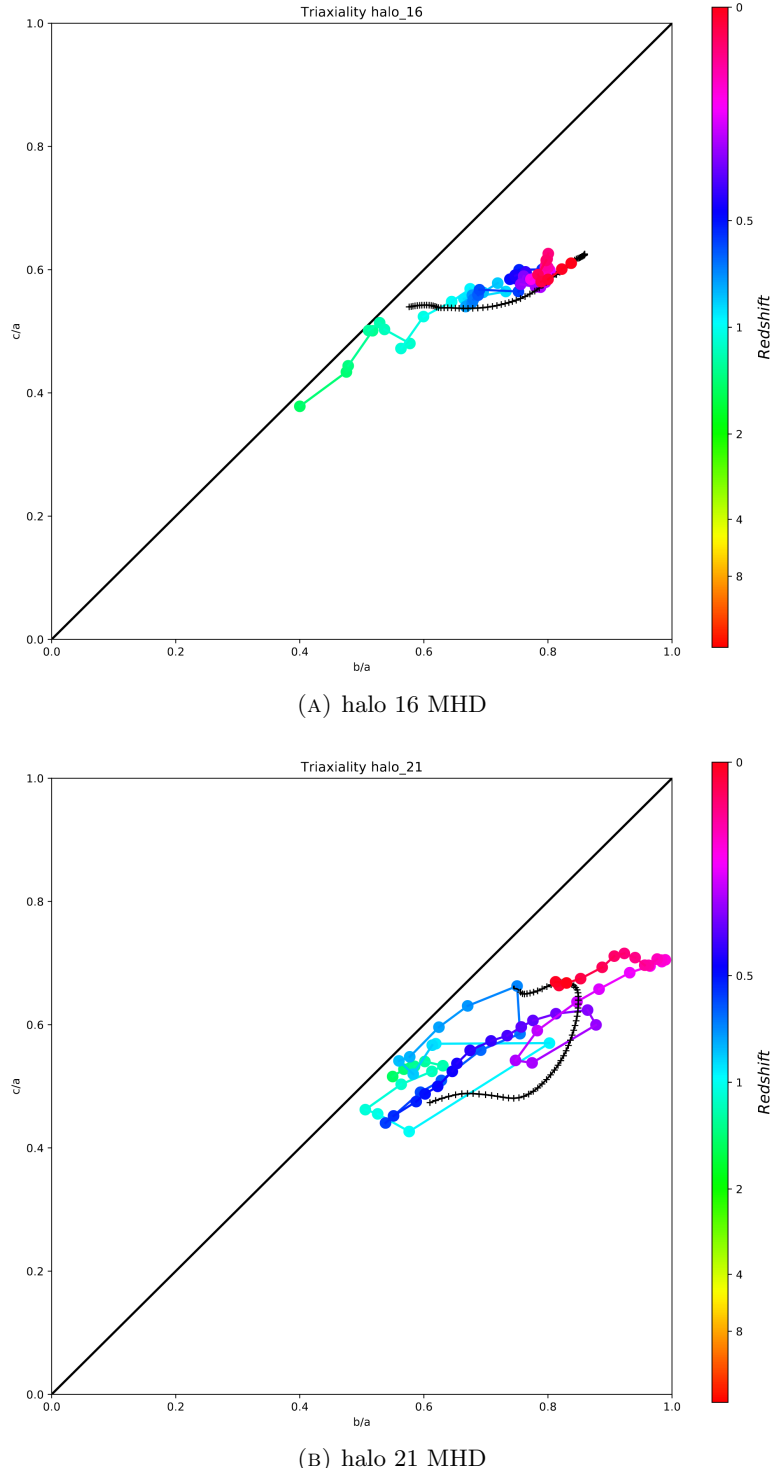


FIGURE 3.10: Historic shape Vs radial shape on the Triaxiality plane. The black line represents the radial profile at redshift 0. The colored connected dots represent the shape measured at the virial radius $R_{\text{Mean}} 200$ at a certain redshift (color)

Chapter 4

Conclusions

Conclusions

Appendix A

An Appendix

Lorem ipsum dolor sit amet, consectetur adipiscing elit. Vivamus at pulvinar nisi. Phasellus hendrerit, diam placerat interdum iaculis, mauris justo cursus risus, in viverra purus eros at ligula. Ut metus justo, consequat a tristique posuere, laoreet nec nibh. Etiam et scelerisque mauris. Phasellus vel massa magna. Ut non neque id tortor pharetra bibendum vitae sit amet nisi. Duis nec quam quam, sed euismod justo. Pellentesque eu tellus vitae ante tempus malesuada. Nunc accumsan, quam in congue consequat, lectus lectus dapibus erat, id aliquet urna neque at massa. Nulla facilisi. Morbi ullamcorper eleifend posuere. Donec libero leo, faucibus nec bibendum at, mattis et urna. Proin consectetur, nunc ut imperdiet lobortis, magna neque tincidunt lectus, id iaculis nisi justo id nibh. Pellentesque vel sem in erat vulputate faucibus molestie ut lorem.

Quisque tristique urna in lorem laoreet at laoreet quam congue. Donec dolor turpis, blandit non imperdiet aliquet, blandit et felis. In lorem nisi, pretium sit amet vestibulum sed, tempus et sem. Proin non ante turpis. Nulla imperdiet fringilla convallis. Vivamus vel bibendum nisl. Pellentesque justo lectus, molestie vel luctus sed, lobortis in libero. Nulla facilisi. Aliquam erat volutpat. Suspendisse vitae nunc nunc. Sed aliquet est suscipit sapien rhoncus non adipiscing nibh consequat. Aliquam metus urna, faucibus eu vulputate non, luctus eu justo.

Donec urna leo, vulputate vitae porta eu, vehicula blandit libero. Phasellus eget massa et leo condimentum mollis. Nullam molestie, justo at pellentesque vulputate, sapien velit ornare diam, nec gravida lacus augue non diam. Integer mattis lacus id libero ultrices sit amet mollis neque molestie. Integer ut leo eget mi volutpat congue. Vivamus sodales, turpis id venenatis placerat, tellus purus adipiscing magna, eu aliquam nibh dolor id nibh. Pellentesque habitant morbi tristique senectus et netus et malesuada fames ac turpis egestas. Sed cursus convallis quam nec vehicula. Sed vulputate neque eget odio fringilla ac sodales urna feugiat.

Phasellus nisi quam, volutpat non ullamcorper eget, congue fringilla leo. Cras et erat et nibh placerat commodo id ornare est. Nulla facilisi. Aenean pulvinar scelerisque eros eget interdum. Nunc pulvinar magna ut felis varius in hendrerit dolor accumsan. Nunc pellentesque magna quis magna bibendum non laoreet erat tincidunt. Nulla facilisi.

Duis eget massa sem, gravida interdum ipsum. Nulla nunc nisl, hendrerit sit amet commodo vel, varius id tellus. Lorem ipsum dolor sit amet, consectetur adipiscing elit. Nunc ac dolor est. Suspendisse ultrices tincidunt metus eget accumsan. Nullam facilisis, justo vitae convallis sollicitudin, eros augue malesuada metus, nec sagittis diam nibh ut sapien. Duis blandit lectus vitae lorem aliquam nec euismod nisi volutpat. Vestibulum ornare dictum tortor, at faucibus justo tempor non. Nulla facilisi. Cras non massa nunc, eget euismod purus. Nunc metus ipsum, euismod a consectetur vel, hendrerit nec nunc.

Bibliography

- [] J. M. Bardeen, J. R. Bond, N. Kaiser, and A. S. Szalay. The statistics of peaks of Gaussian random fields. *APJ*, 304:15–61, May 1986. doi: 10.1086/164143.
- [] C. Nipoti, P. Londrillo, H. Zhao, and L. Ciotti. Vertical dynamics of disc galaxies in modified Newtonian dynamics. *MNRAS*, 379:597–604, August 2007. doi: 10.1111/j.1365-2966.2007.11835.x.
- [] J. I. Read and Ben Moore. Tidal streams in a mond potential: constraints from sagittarius. *MNRAS*, 361(3):971–976, 2005. doi: 10.1111/j.1365-2966.2005.09232.x.
URL [+http://dx.doi.org/10.1111/j.1365-2966.2005.09232.x](http://dx.doi.org/10.1111/j.1365-2966.2005.09232.x).
- [] J. I. Read, G. Lake, O. Agertz, and Victor P. Debattista. Thin, thick and dark discs in cdm. *MNRAS*, 389(3):1041–1057, 2008. doi: 10.1111/j.1365-2966.2008.13643.x.
URL [+http://dx.doi.org/10.1111/j.1365-2966.2008.13643.x](http://dx.doi.org/10.1111/j.1365-2966.2008.13643.x).
- [] J.I. Read, L. Mayer, A.M. Brooks, F. Governato, and G. Lake. A dark matter disc in three cosmological simulations of Milky Way mass galaxies. *MNRAS*, 397:44–51, July 2009. doi: 10.1111/j.1365-2966.2009.14757.x.
- [] C.A. Vera-Ciro, L.V. Sales, A. Helmi, C.S. Frenk, J.F. Navarro, V. Springel, M. Vogelsberger, and S.D.M. White. The shape of dark matter haloes in the Aquarius simulations: evolution and memory. *MNRAS*, 416:1377–1391, September 2011. doi: 10.1111/j.1365-2966.2011.19134.x.
- [] R. J. J. Grand, F. A. Gomez, F. Marinacci, R. Pakmor, V. Springel, D. J. R. Campbell, C. S. Frenk, A. Jenkins, and S. D. M. White. The Auriga Project: the properties and formation mechanisms of disc galaxies across cosmic time. *MNRAS*, 467:179–207, May 2017. doi: 10.1093/mnras/stx071.
- [] V. Springel. E pur si muove: Galilean-invariant cosmological hydrodynamical simulations on a moving mesh. *MNRAS*, 401:791–851, January 2010. doi: 10.1111/j.1365-2966.2009.15715.x.

- B. Allgood, R. A. Flores, J. R. Primack, A. V. Kravtsov, R. H. Wechsler, A. Faltenbacher, and J. S. Bullock. The shape of dark matter haloes: dependence on mass, redshift, radius and formation. *MNRAS*, 367:1781–1796, April 2006. doi: 10.1111/j.1365-2966.2006.10094.x.